Jan Pech

2D simulation of flow behind a heated cylinder using spectral element approach with variable coefficients

In: Jan Chleboun and Petr Přikryl and Karel Segeth and Jakub Šístek and Tomáš Vejchodský (eds.): Programs and Algorithms of Numerical Mathematics, Proceedings of Seminar. Dolní Maxov, June 8-13, 2014. Institute of Mathematics AS CR, Prague, 2015. pp. 169–174.

Persistent URL: http://dml.cz/dmlcz/702680

Programs and Algorithms of Numerical Matematics 17
J. Chleboun, P. Přikryl, K. Segeth, J. Šístek, T. Vejchodský (Eds.)
Institute of Mathematics AS CR, Prague 2015

2D SIMULATION OF FLOW BEHIND A HEATED CYLINDER USING SPECTRAL ELEMENT APPROACH WITH VARIABLE COEFFICIENTS

Jan Pech[1,2]

[1] New Technologies-Research Center, University of West Bohemia in Pilsen
Universitní 8, 30614 Pilsen, Czech Republic
[2] Institute of Thermomechanics, Academy of Sciences of the Czech Republic
Dolejškova 1402/5, 182 00 Praha 8, Czech Republic
jpech@it.cas.cz

Abstract

The scheme for the numerical solution of the incompressible Navier-Stokes equations coupled with the equation for temperature through the temperature dependent viscosity and thermal conductivity coefficients is presented. It is applied, together with the spectral element method, to the 2D calculations of flow around heated cylinder. High order polynomial approximation is combined with the decomposition of whole computational domain to only a few elements. Resulting data are compared with the experimental data.

1. Introduction

The viscosity and the thermal conductivity of water and air depend on the temperature. As a consequence, a wake behind an obstacle in an isothermal setting differs from the situation, when the body and the fluid temperatures do not coincide. The experimental data, see [5], for the flow around the heated cylinder are available for both water and air in the flow regimes exhibiting regular vortex shedding. The cited experimental data are available for Reynolds numbers ($Re = DV_\infty/\nu_\infty$) in the range $50 < Re < 170$, when Re is related to the cylinder diameter D (V_∞ is the upstream velocity magnitude and ν_∞ is the upstream value of the kinematic viscosity). The conditions and flow parameters in the mentioned experiment were such, that the compressibility of both water and air can be neglected. Therefore the fluid density (ρ) may be assumed to be a constant and the incompressible model will be used. The system of equations describing the heated flow consists of the Navier-Stokes equations (1) with the incompressible constraint (2)

$$\frac{\partial \vec{v}}{\partial t} + \vec{v} \cdot \nabla \vec{v} = -\nabla p + \nabla \cdot \left[\nu \left(\nabla \vec{v} + (\nabla \vec{v})^{\mathbf{T}} \right) \right] , \tag{1}$$

$$\nabla \cdot \vec{v} = 0 \tag{2}$$

and the convection-diffusion equation for temperature (T):

$$\rho c_p \left(\frac{\partial T}{\partial t} + \vec{v} \cdot \nabla T \right) = \nabla \cdot (\lambda \nabla T) \ , \tag{3}$$

where in the system (1)-(3) $\vec{v}$ denotes the fluid velocity vector, p is the kinematic pressure, λ the thermal conductivity and the constant c_p is the specific heat at the constant pressure. Due to the nature of the pressure in the incompressible models the above system is complete without the equation of state, on the other hand the variability of the material coefficients causes strong coupling of equations (1) and (3). The thermal dependencies of ν and λ can be approximated by power function obtained from a tabulated data as in [3]:

$$\nu(T) = \nu_\infty (T/T_\infty)^{\omega_\nu} \ , \text{(air: } \omega_\nu = 0.7774, \text{ water: } \omega_\nu = -7 \text{)}, \tag{4}$$

$$\lambda(T) = \lambda_\infty (T/T_\infty)^{\omega_\lambda} \ , \text{(air: } \omega_\lambda = 0.85, \text{ water: } \omega_\lambda = 0.71 \text{)}, \tag{5}$$

where $1 \leq (T/T_\infty) \leq \tilde{T} = (T_W/T_\infty)$ (T_W is the constant temperature of the cylinder wall).

The system of equations (1)-(3) generally admits non-smooth or even discontinuous solutions, but observations do not confirm any shocks in the mentioned range of Re for the fluids in the state which coincides with description in [5]. This suggests possible existence of a smoother solution. Therefore we will use the computational method based on the assumption of smooth data and solution, as is the spectral method (see e.g. [2]). This method converges with increasing (e.g. polynomial) order of the expansion basis. If the method is applicable, its minimization of the number of degrees of freedom and the convergence rate are superior to methods of lower, fixed order, which converge by dividing the computational domain to smaller parts. On the other hand, spectral methods are not always applicable. Already the fact, that the cylinder is in our case represented as a circular hole inside the domain, forces us to leave pure spectral method and use the spectral element method, which combines the geometrical flexibility of the finite element method with the approach of the spectral method. This leads us to use of minimal number of elements and application of very high order expansion basis. However, the class of equations where the high orders are advantageous for numerical computation is limited and this fact must be taken into account in design of the numerical scheme.

2. Numerical scheme

The numerical scheme for the system (1)–(3) was developed on the base of the splitting scheme for the Navier-Stokes equations with a variable viscosity ([1]), where the temperature dependent viscosity was decomposed to the sum of the constant ν_∞ and the variable part ν_s: $\nu(T(\vec{x},t)) = \nu_\infty + \nu_s(\vec{x},t)$. Denoting by " ˆ " and " ˜ "

intermediate fields, by superscript the values of the variables in the n-th time level and by Δt the time step, we arrive to the first order scheme in time (see [4]):

$$\frac{\hat{\vec{v}} - \vec{v}^n}{\Delta t} = -(\vec{v}^n \cdot \nabla)\vec{v}^n + \nabla \cdot [\nu_s^n (\nabla \vec{v}^n + \nabla^T \vec{v}^n)] \ , \tag{6}$$

$$\frac{\tilde{\vec{v}} - \hat{\vec{v}}}{\Delta t} = -\nabla p^{n+1} \underbrace{\Rightarrow}_{\nabla \cdot \tilde{\vec{v}} = 0} \nabla^2 p^{n+1} = \nabla \cdot \left(\frac{\hat{\vec{v}}}{\Delta t} \right) \ , \tag{7}$$

$$\frac{\vec{v}^{n+1} - \tilde{\vec{v}}}{\Delta t} = \nu_\infty \nabla \cdot \nabla \vec{v}^{n+1} \ . \tag{8}$$

The key role plays the high order pressure boundary condition (HOPBC), which is asserted on the boundaries, where the Dirichlet condition for velocity is prescribed:

$$\frac{\partial p^{n+1}}{\partial \vec{n}} = \vec{n} \cdot \left[-(\vec{v}^n \cdot \nabla)(\vec{v}^n) + \nabla \cdot \left(\nu^n \nabla \vec{v}^n + \nu^n (\nabla \vec{v}^n)^{\mathbf{T}} \right) \right] \ . \tag{9}$$

Temperature dependence of the thermal conductivity is needed to keep the correct Prandtl number ($Pr = \nu \rho c_p / \lambda$). The scheme for the temperature equation was derived again by the operator splitting combined with the splitting of λ to the constant λ_∞ and the variable part λ_s, i.e. $\lambda(T(\vec{x}, t)) = \lambda_\infty + \lambda_s(\vec{x}, t)$.

The operator splitting then allows the implicit treatment of the diffusion operator with the constant coefficient (λ_∞) and the explicit treatment of the part with the variable conductivity (λ_s). The first order scheme in time for temperature reads:

$$\frac{\hat{T} - T^n}{\Delta t} = -(\vec{v}^n \cdot \nabla) T^n - \frac{1}{\rho c_p} \nabla \cdot (\lambda_s^n \nabla T^n) \ . \tag{10}$$

As in (7) and (8) the spectral element method is applicable to the implicit step of the scheme for temperature:

$$\frac{\lambda_\infty}{\rho c_p} \nabla^2 T^{n+1} - \frac{T^{n+1}}{\Delta t} = -\frac{\hat{T}}{\Delta t} \ . \tag{11}$$

The whole scheme (6)–(11) was implemented on the base of the modified Nektar++ library of version 3.3.0 and the deeply modified incompressible Navier-Stokes solver provided with the same library.

3. Mesh and parameters of the computation

The model assumed the flow in an open channel, which is not significantly influenced by a tank walls (in experiment) or Dirichlet boundary conditions on outer boundaries (in computation). Therefore the dimensions of the computational domain must be large enough. The cylinder diameter $D = 1$ was chosen for simplicity and then the spatial dimensions of the computational domain were: $20D$ upstream,

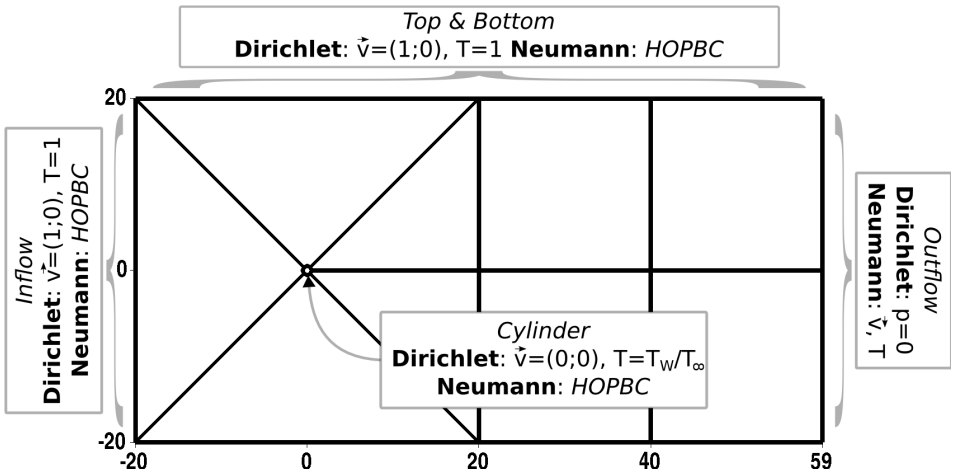

Figure 1: The computational mesh consisting of 9 elements with description of the boundary conditions (*HOPBC* is given by eq. (9)). The curve of the cylinder wall was given by 10^{th} order polynomial for each of the adjacent elements.

$60D$ downstream and $20D$ above and under the cylinder. We divided the computational domain to small number of elements ($NEL = 9$) and used the rich expansion basis, having polynomial orders up to $p = 49$ in each coordinate variable (2500 DOFs per element). The *no slip* condition and value of relative temperature $\tilde{T}$ was prescribed at the cylinder wall. Figure 1 shows the boundary conditions and the computational mesh with all its elements. The chosen values of the inlet boundary conditions imply $\nu_\infty = 1/Re$ and $\lambda_\infty/(\rho c_p) = 1/(RePr)$, so we can set Re and Pr as independent, dimensionless parameters and avoid the explicit specification of the constants ρ and c_p. The initial conditions for both velocity and temperature were constants equal to the values on the inflow boundary. The final quantity for the comparison with the experimental results was the *Strouhal number* $St = fD/V_\infty$ (f denotes here the frequency of the vortex shedding). The effects of the heating as a relation of St, Re and Pr numbers was studied also theoretically, see the empirical formula derived in [3], which shall also be used for the comparison with the results of the computation.

4. Results

The value of the Strouhal number can be determined from the temporal oscilations of the approximative values of the forces acting on the cylinder. These forces are often denoted as *lift* and *drag* force. As the flow develops to the von Kármán vortex street, the oscillations tend to stable frequency. The stabilized periodicity was recognized in the data and the averaged frequency through multiple periods was computed (see Figure 3). Since the flow develops slowly from the constant initial conditions, a long time computation was needed (about 300000 time steps $\Delta t = 0.001$, depending on the Reynolds number).

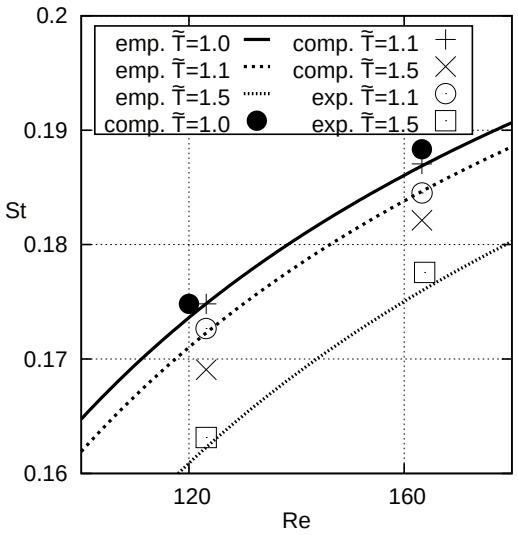

Figure 2: The resulting dependence of Strouhal number on Reynolds number for various temperatures ($\tilde{T} = T_W/T_\infty$) and flow of air.

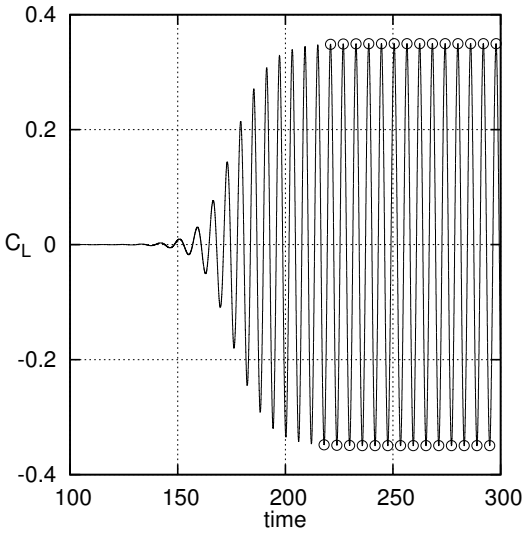

Figure 3: Plot of the lift coefficient C_L for $Re = 123.2$, $T_W/T_\infty = 1.5$ in the flow of air. Rings indicate the extremes taken for computation of the Strouhal number.

The resulting graphs of $St - Re$ dependencies for both air and water, for various cylinder temperatures, is shown in Fig. 2 and Fig. 4. The continuous curve is given by the empirically obtained formula, see [3].

5. Conclusion

The presented results demonstrate applicability of the computational scheme (6)–(11) introduced in combination with high order spatial approximation. Obtained $St - Re$ dependencies show qualitatively good agreement with the experimental results ([5, 3]) across various cylinder temperatures. Observed shift of the data is mostly caused by insufficient expansion basis, since the expansion coefficients of the highest orders were converged only to the values around 0.01. This setting of the expansion basis was chosen due to high memory demands of the matrix system of reference computations, since the work was performed on single CPU.

The increase/decrease of the Strouhal number caused by heating is smaller than predictions of both the experiment and the empirical formula. On the other hand, in case of water flow, the differences of the experiment from the empirical formula are on the same level as the error of the computation.

The results are well comparable with standard approaches using hundreds of thousands low order elements. The main advantage of the spectral approach stays in the significant reduction of number of DOFs and possible reaching of exponential error decay. Achievement of more accurate solutions will be the goal of future computations.

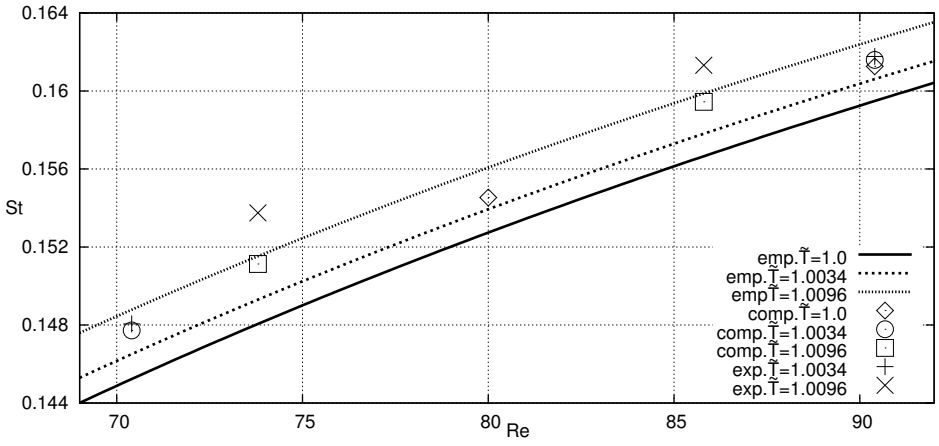

Figure 4: Resulting $St - Re$ dependence for various temperatures in flow of water.

Acknowledgements

The result was developed within the CENTEM project, no. CZ.1.05/2.1.00/ 03.0088, co-funded by the ERDF as part of the Ministry of Education, Youth and Sports OP RDI programme.

References

[1] Karamanos, G. and Sherwin, S.: A high order splitting scheme for the Navier-Stokes equations with variable viscosity. Applied Numerical Mathematics **33** (2000), 455–462.

[2] Karniadakis, G. and Sherwin, S.: *Spectral/hp element methods for computational fluid dynamics.* Oxford University Press, 2005.

[3] Maršík, F., Trávníček, Z., Yen, R., Tu, W., and Wang, A.: Sr-Re-Pr relationship for a heated/cooled cylinder in laminar cross flow. In: *Proceedings of CHT-08 ICHMT International Symposium on Advances in Computational Heat Transfer*, 2008.

[4] Pech, J. and Maršík, F.: 2D simulation of flow around heated circular cylinder with variable viscosity using high order spectral elements. In: *Proceedings of Conference Topical Problems of Fluid Mechanics 2014*, pp. 89–92, 2014.

[5] Vít, T., Ren, M., Trávníček, Z., Maršík, F., and Rindt, C.: The influence of temperature gradient on the Strouhal–Reynolds number relationship for water and air. Experimental Thermal and Fluid Science **31** (2007), 751–760.